Wave-vector dependent intensity variations of the Kondo peak in photoemission from $CePd_3$

S. Danzenbächer,[1] Yu. Kucherenko,[2] M. Heber,[1,*] D. V. Vyalikh,[1] S. L. Molodtsov,[1] V. D. P. Servedio,[1,†] and C. Laubschat[1]
[1]*Institut für Festkörperphysik, TU Dresden, D-01062 Dresden, Germany*
[2]*Institute of Metal Physics, National Academy of Sciences of Ukraine, UA-03142 Kiev, Ukraine*
(Received 6 May 2005; published 13 July 2005)

Strong angle-dependent intensity variations of the Fermi-level feature are observed in the $4d \rightarrow 4f$ resonant photoemission spectra of $CePd_3(111)$, that reveal the periodicity of the lattice and largest intensity close to the $\bar{\Gamma}$ points of the surface Brillouin zone. In the framework of a simplified periodic Anderson model the phenomena may quantitatively be described by a wave-vector dependence of the electron hopping matrix elements caused by Fermi-level crossings of non-$4f$-derived energy bands.

DOI: 10.1103/PhysRevB.72.033104 PACS number(s): 71.20.Eh, 71.27.+a, 79.60.−i

In Ce compounds, the interaction of localized $4f$ states with itinerant valence-band (VB) states may lead to a number of fascinating phenomena ranging from valence instabilities to heavy-fermion and even non-Fermi-liquid behavior.[1] Although part of the physical properties of these compounds may be understood in the framework of local-density approximation (LDA) band-structure calculations, the latter are not able to account properly for the correlated nature of the f electrons. For the latter, localized approaches are applied based on the Kondo or Anderson Hamiltonians. Particularly, the application of the single-impurity Anderson model (SIAM)[2] was very successful, allowing a quantitative correlation of transport, thermodynamic, and magnetic properties of the materials with spectroscopic data (see, for example, Ref. 3). A shortcoming of this model, however, is its restriction to an isolated f impurity that ignores the influence of the periodicity of the lattice on the f state. Anisotropies of physical properties, therefore, are usually only discussed in terms of crystal field effects, while a **k** dependence of hybridization is not considered.[4] Taking this into account, the latter leads to the periodic Anderson model (PAM) for which, however, realistic approaches are presently still missing.[5]

Experimentally, in particular, angle-resolved photoemission (PE) has been used to search for inconsistencies of SIAM that make the use of the PAM necessary. In PE spectra, the Ce $4f$ emissions reveal a characteristic double peak structure consisting of a spin-orbit split Fermi-level (E_F) feature related to the Kondo resonance and a broad peak at about 2 eV binding energy (BE) that corresponds roughly to the $4f^0$ final state expected for photoionization of a $4f^1$ ground state. In light of the PAM, BE and intensity variations of these features as a function of electron wave vector **k** are expected to be particularly strong for the Fermi-level peak. In fact, in a few cases energy dispersions[6–11] and **k**-dependent intensity variations[6,10,12] were reported and qualitatively interpreted in light of the PAM. A quantitative description of the phenomena in relation to the VB structure, however, is still lacking.

In this contribution we report on an angle-resolved $4d \rightarrow 4f$ resonant PE study of $CePd_3(111)$. This compound is characterized by a relatively low VB density of states around the Fermi energy[13] and band crossings of the Fermi level may only be observed by photoemission at certain points in **k** space. $CePd_3(111)$ represents, therefore, an ideal system for the search of **k** dependencies of the $4f$ emission. While BE variations of the individual spectral $4f$ components are found to be not larger than 30 meV, strong **k**-dependent intensity variations of the Fermi-level feature with respect to the intensity of the ionization peak are observed. These variations reflect the periodicity of the lattice and reveal the largest intensity close to the $\bar{\Gamma}$ points of the surface Brillouin zones (BZ). The phenomenon is analyzed in the framework of a simplified PAM, where the less probable on-site double occupation of $4f$ states is neglected in order to achieve **k** conservation upon interaction. In this case, the intensity of the Fermi-level feature is directly related to the dispersive properties of the VB states and becomes particularly large at those points of **k** space, where the BE of the VB states approaches E_F. Taking VB dispersions from LMTO-slab calculations, good agreement between theory and experiment is achieved.

Angle-resolved resonant PE experiments at the $4d \rightarrow 4f$ absorption threshold were performed with synchrotron radiation provided by the U49/2-PGM-1 undulator beamline of BESSY II. A hemispherical Thermo-VG CLAM-IV analyzer tuned to an energy resolution of 25 meV (FWHM) and an angular resolution of better than 1° was used. Epitaxial $CePd_3$ films with thicknesses of approximately 100 Å were grown on a clean W(110) substrate by thermal deposition of stoichiometric amounts of Pd and Ce and subsequent annealing.[13] The resulting LEED pattern revealed a sharp (2×2) overstructure with respect to the spots of a pure Pd(111) film, as expected for the (111) surface of $CePd_3$ (cubic $AuCu_3$ structure).[13] During vapor deposition as well as for the PE experiments the substrate temperature was held below 90 K. The base pressure in the ultrahigh vacuum system was in the upper 10^{-11}-mbar range and raised only shortly to 1×10^{-9} mbar during sample preparation. Oxygen and carbon contaminations were checked monitoring the respective VB signals and found to be negligible.

Figure 1 shows a three-dimensional plot of a series of on-resonance PE spectra taken at 121 eV photon energy and different emission angles corresponding to a variation of the parallel component of the **k** vector along the $\bar{\Gamma}-\bar{K}-\bar{M}-\bar{K}-\bar{\Gamma}$ direction in the surface BZ. At this photon energy the $4f$ photoemission cross section is strongly enhanced by a Fano

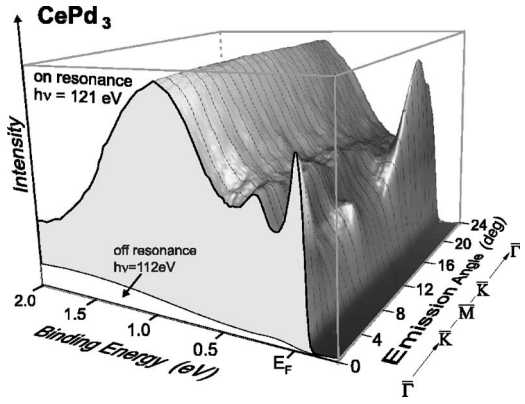

FIG. 1. Experimental on-resonance PE spectra of $CePd_3$ taken at the $4d \rightarrow 4f$ excitation threshold ($h\nu$=121 eV) at different emission angles (θ) and normalized to the maximum intensity of the ionization peak. The subspectrum illustrates valence-band contributions as observed off-resonance at 112 eV photon energy, normalized to the same photon flux as the corresponding on-resonance spectrum (θ=0°).

resonance, while contributions from the VB emissions are negligibly small due to a Cooper minimum of the Pd $4d$ cross section. The latter is illustrated in Fig. 1 by the blank subspectrum area, which shows the VB signal in normal emission geometry observed at the Fano off-resonance ($h\nu$ =112 eV) normalized to the same photon flux as the corresponding on-resonance spectrum. The on-resonance spectra are normalized to the maximum intensity of the ionization peak. The Fermi-level peak reveals large intensity close to the $\bar{\Gamma}$ point. Upon leaving the $\bar{\Gamma}$-point region, the intensity decreases strongly and arrives again at a small local maximum in the region of the $\bar{M}$ point. The spin-orbit split sideband at about 300 meV BE, on the other hand, reveals almost constant intensity and increases its BE by about 30 meV when going from $\bar{\Gamma}$ to $\bar{M}$. Thus, the intensity variation of the Fermi-level peak cannot be ascribed to photoelectron diffraction effects, but reflects an intrinsic electronic property. Similarly, although less dramatic effects have been reported for $CePt_{2+x}$[10,12] and $CeBe_{13}$,[6] where the intensity variations were tentatively ascribed to a dispersing band that crosses the Fermi energy[12] or a **k**-vector dependence of hybridization.[10]

The starting point of our analysis of the measured PE spectra is the PAM:

$$H = \sum_{\mathbf{k},\sigma} \varepsilon(\mathbf{k}) d^{+}_{\mathbf{k}\sigma} d_{\mathbf{k}\sigma} + \sum_{\mathbf{k},\sigma} \varepsilon_f(\mathbf{k}) f^{+}_{\mathbf{k}\sigma} f_{\mathbf{k}\sigma} + \sum_{\mathbf{k},\sigma} V_{\mathbf{k}}(\varepsilon)(d^{+}_{\mathbf{k}\sigma} f_{\mathbf{k}\sigma} + f^{+}_{\mathbf{k}\sigma} d_{\mathbf{k}\sigma}) + \frac{U_{ff}}{2} \sum_{i,\sigma} n^{f}_{i,\sigma} n^{f}_{i,-\sigma} = \sum_{\mathbf{k}} h_0(\mathbf{k}) + u, \quad (1)$$

where the extended VB states $|\mathbf{k}\sigma\rangle$ have a dispersion $\varepsilon(\mathbf{k})$ and are described by creation (annihilation) operators $d^{+}_{\mathbf{k}\sigma}$ ($d_{\mathbf{k}\sigma}$). The operator $f^{+}_{\mathbf{k}\sigma}$ creates an f electron with momentum **k**, spin σ, and energy $\varepsilon_f(\mathbf{k})$. We assume that a nonhybridized f band has no dispersion: $\varepsilon_f(\mathbf{k})=\varepsilon_f$. The two electron subsystems (VB and f states) are coupled via a hybridization $V_{\mathbf{k}}(\varepsilon)$, and, finally, U_{ff} is the Coulomb repulsion between two f electrons localized on the same lattice site. The transformation of the latter term to a **k** representation leads to a mixing of states with different **k** values, which makes the problem difficult to handle quantitatively. However, if U_{ff} is sufficiently large with respect to $|\varepsilon_f|$ and $V_{\mathbf{k}}$, contributions of the $4f^2$ configuration to the ground and excited states become negligibly small as compared to contributions of the $4f^0$ and $4f^1$ configurations. In fact, this condition is roughly fulfilled for Ce transition-metal compounds. In these systems U_{ff} amounts to 7 eV, while $|\varepsilon_f|$ is of the order of 1 eV and the hybridization parameter is even less than $|\varepsilon_f|$.[3,14] For $U_{ff} \rightarrow \infty$ the probability to find two f electrons localized on the same site becomes zero, and the problem could be solved by diagonalizing the Hamiltonian $h_0(\mathbf{k})$ that describes a coupling of an f electron with the energy ε_f to VB states with a specific wave vector **k**. In this way the problem formally reduces to the one of SIAM with the only difference being that the density of states (DOS) used in SIAM is now replaced by a **k**-dependent energy distribution of states.[14] Since the results of SIAM are usually not strongly affected by the neglecting of $4f^2$ contributions, one may expect that at least qualitatively our model leads to a correct description of the experimental data.

As a first step of our theoretical treatment we performed calculations of the VB structure of $CePd_3$ by means of the LMTO method.[15] In the calculations Ce was replaced by La in order to suppress contributions of Ce $4f$ states to the VB DOS. The second step was the calculation of the spectral function using the simplified PAM, as described above. Values taken directly from the band-structure calculations were the energies of the valence bands $\varepsilon(\mathbf{k})$ as well as the coefficients $c_l(\varepsilon,\mathbf{k})$ of the l-projected local expansion of the Bloch functions at the La site. Due to symmetry requirements, the localized $4f$ states couple only to those VB states that reveal non-negligible local f contributions inside the rare-earth atomic sphere. Consequently, the hybridization matrix element was chosen to be proportional to the respective coefficients:

$$V_{\mathbf{k}}(\varepsilon) = \Delta \cdot c_f(\varepsilon,\mathbf{k}), \quad (2)$$

whereby Δ (like ε_f) is treated as a constant, but adjustable, parameter.

In the kinetic energy range of the experiment ($\sim$115 eV) the mean-free path of the photoelectrons amounts to only $\sim$4.5 Å (Ref. 16). In order to account for surface effects in the VB DOS, we calculated the electronic structure of a five-layer slab constructed from (111) atomic planes. Then, the PE spectral functions were simulated as a superposition of weighted contributions from different atomic layers, where the third atomic layer (in the middle of the slab) was considered as bulk. The weights were estimated to be equal to 0.41 for the surface layer, 0.24 for the second layer, and 0.35 for the bulk, assuming an exponential dependence of the photoelectron escape probability.

Figure 2 shows the f contributions to the local DOS of $LaPd_3$(111) along the $\bar{\Gamma}-\bar{K}-\bar{M}$ direction in the surface BZ for the outermost atomic layer. Near the $\bar{\Gamma}$-point energy bands crossing E_F are mainly derived from Pd p states with

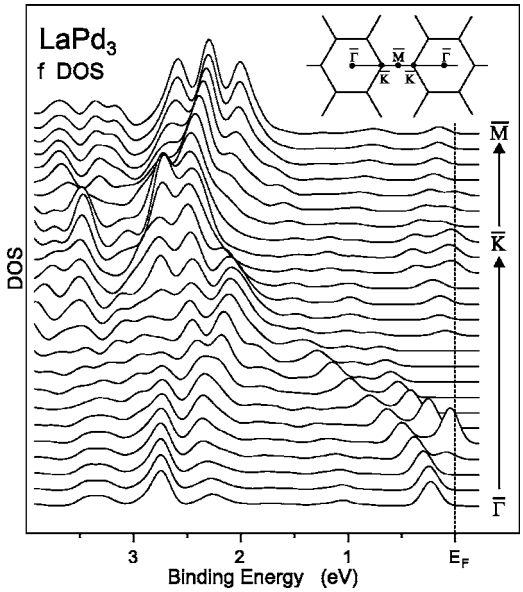

FIG. 2. Local f DOS ($|c_f(\varepsilon,\mathbf{k})|^2$ values broadened by a Gaussian of 0.2 eV FWHM) inside the La atomic sphere of a $LaPd_3(111)$ surface layer calculated for different points along the $\bar{\Gamma}-\bar{K}-\bar{M}$ direction of the surface BZ. The results are almost independent from the actual choice of the wave-vector component perpendicular to the surface, since the dispersion of energy bands is found to be negligibly small in this direction.

a noticeable admixture of La and Pd d states. At the La site, these bands reveal a finite f character. Halfway between $\bar{\Gamma}$ and $\bar{K}$, no bands are found just below E_F. In the vicinity of the BZ borders, however, bands appear again in this energy region. Near the $\bar{K}$ point as well as between the $\bar{K}$ and $\bar{M}$ points, weak f contributions to the local DOS are visible. The respective bands are mainly derived from La d as well as Pd p and d states. Strong peaks below 2 eV BE are related to Pd $4d$ derived bands that also show a finite f character at the La sites.

Calculated $4f$ spectral functions for the $\bar{\Gamma}$ and $\bar{K}$ points are presented in Fig. 3 in comparison with the experimental data. The spectral functions were obtained using similar parameter values as in SIAM:[14,17] $\varepsilon_f=1.30$ eV and $\Delta=0.86$ eV (for the surface atomic layer, ε_f was assumed to be shifted by 0.20 eV to higher BE). An energy-dependent lifetime broadening parameter in the form $\Gamma_L(E)=0.01$ eV $+0.12E$ was used, where E denotes the BE with respect to E_F. The calculated spectra were additionally broadened with a Gaussian ($\Gamma_G=0.03$ eV) to simulate finite instrumental resolution and an integral background was added to take into account inelastic scattering events. Close to the $\bar{\Gamma}$ point, the strong VB f contributions near E_F lead to a large (spin-orbit split) peak at E_F, whereas in the spectra at the $\bar{K}$ point only two shoulders are obtained in this energy region due to the reduced f character of the respective VB states. For $\mathbf{k}$ points, where the VB f contributions near E_F are negligible, this spectral structure disappears.

As evident from Fig. 2, there is a Fermi-level crossing of a second band at about 25% of the $\bar{\Gamma}-\bar{K}$ distance that should

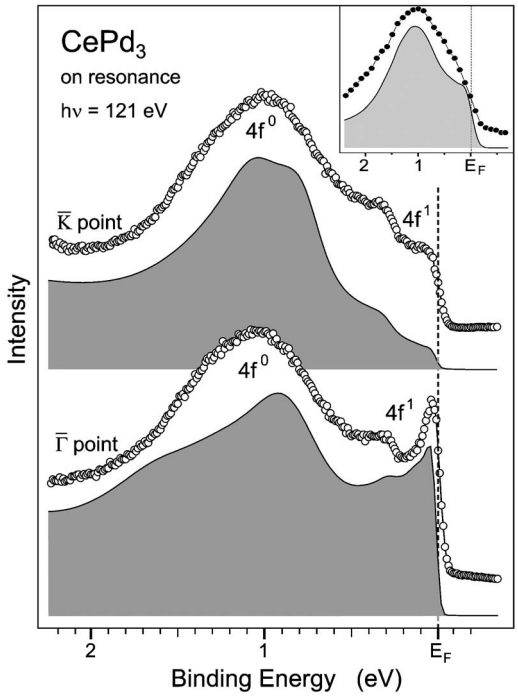

FIG. 3. Calculated $4f$ spectral functions (shadowed subspectra: $U_{ff}=\infty$, $\Delta=0.86$ eV) for the $\bar{\Gamma}$ and $\bar{K}$ points in comparison with the experimental data (open circles). The inset shows the angle-integrated spectrum of $CePd_3$ together with the simulations within SIAM from Ref. 17, where the peak at E_F is not observed, since it appears only at certain $\mathbf{k}$ points.

lead to an even larger Fermi-level peak at this $\mathbf{k}$ point than around the $\bar{\Gamma}$ point. Apart from the fact that the respective angular deviation (1.5° at $h\nu=121$ eV) is in the order of the accuracy of our experiment, a rigid shift of E_F by 0.2 eV to a lower or higher BE would dispose of this discrepancy. Energy shifts of this order of magnitude may be caused by variations of the potential in the rare-earth atomic sphere caused, e.g., by the substitution of Ce by La in the electronic structure calculations.

In the calculated spectra, dispersive substructures appearing in the region of the ionization peak are not observed in the experimental data. The substructures reflect interactions of the ionized $4f$ state with VB states of the same BE and are only weakly related to the ground state properties of the system.[18] At least part of the observed discrepancy may be attributed to the neglecting of the f-f correlation term: First, a finite value of U_{ff} would lead to a certain integration over $\mathbf{k}$ space and a smearing-out of substructures. The same mechanism would also cause the appearance of finite Fermi-level features, even at $\mathbf{k}$ points, where no VB states are found close to E_F, in agreement with the experiment. Second, the neglecting of the correlation term leads to an overestimation of Δ, since contributions to the Fermi-level peak, that are due to direct $4f^2\rightarrow 4f^1$ photoemission processes, are attributed to $4f^0-4f^1$ configuration interactions. A smaller value of Δ, however, would immediately reduce the dispersion of the ionization-peak substructures.

In conclusion, intensity variations of the Fermi-energy PE peak of $CePd_3$ have been observed that could be related to a

k dependence of hybridization in light of the PAM. Our simple approach has the form of SIAM with a direction-dependent choice of the hybridization $V_{\mathbf{k}}(\varepsilon)$. This suggests that similar approaches may be applied to describe anisotropies in the thermodynamic, magnetic, and transport properties of mixed-valent and heavy-fermion compounds. Reasonable predictions of the **k** dependence of $V_{\mathbf{k}}(\varepsilon)$ may be obtained from LDA band-structure calculations that, like our approach, reveal a large hybridization at those points in **k** space where *f* states are intersected by VB states. Analyses of angle-integrated PE spectra in the light of SIAM are expected to underestimate hybridization strength and overestimate *f* occupation. This is due to the fact that hybridization is particularly large at the Fermi surface where conduction bands cross the Fermi energy while angle-integrated experiments probe also other regions of **k** space that are far away from the Fermi surface and reveal only a small hybridization.

ACKNOWLEDGMENTS

This work was supported by the Deutsche Forschungsgemeinschaft, SFB 463, Projects B2, B4, B11, and B16. Expert assistance by R. Follath and other staff members of BESSY is acknowledged.

*Present address: Freudenberg Dichtungs und Schwingungstechnik KG, Technisches Entwicklungszentrum, D-69465 Weinheim, Germany.

†Present address: Sezione INFM and Dip. di Fisica, Università "La Sapienza," P.le A. Moro 2, 00185 Roma and Centro Studi e Ricerche e Museo della Fisica E. Fermi, Compendio Viminale, Roma, Italy.

[1] G. R. Steward, Rev. Mod. Phys. **73**, 797 (2001).

[2] P. W. Anderson, Phys. Rev. **124**, 41 (1961).

[3] O. Gunnarsson and K. Schönhammer, Phys. Rev. Lett. **50**, 604 (1983); Phys. Rev. B **28**, 4315 (1983); Phys. Rev. B **31**, 4815 (1985).

[4] S. Zhang and P. M. Levy, Phys. Rev. B **40**, 7179 (1989); J. Kitagawa, N. Takeda, M. Ishikawa, T. Yoshida, A. Ishiguro, N. Kimura, and T. Komatsubara, Phys. Rev. B **57**, 7450 (1998).

[5] A. N. Tahvildar-Zadeh, M. Jarrell, and J. K. Freericks, Phys. Rev. Lett. **80**, 5168 (1998); M.-W. Xiao, Z.-Z. Li, and Wang Xu, Phys. Rev. B **65**, 235122 (2002).

[6] A. B. Andrews, J. J. Joyce, A. J. Arko, Z. Fisk, and P. S. Riseborough, Phys. Rev. B **53**, 3317 (1996).

[7] H. Kumigashira, S. H. Yang, T. Yokoya, A. Chainani, T. Takahashi, A. Uesawa, T. Suzuki, O. Sakai, and Y. Kaneta, Phys. Rev. B **54**, 9341 (1996).

[8] H. Kumigashira, S. H. Yang, T. Yokoya, A. Chainani, T. Takahashi, A. Uesawa, and T. Suzuki, Phys. Rev. B **55**, R3355 (1997).

[9] A. J. Arko, J. J. Joyce, A. B. Andrews, J. D. Thompson, J. L. Smith, D. Mandrus, M. F. Hundley, A. L. Cornelius, E. Moshopoulou, Z. Fisk, P. C. Canfield, and A. Menovsky, Phys. Rev. B **56**, R7041 (1997).

[10] M. Garnier, D. Purdie, K. Breuer, M. Hengsberger, and Y. Baer, Phys. Rev. B **56**, R11399 (1997).

[11] J. Boysen, P. Segovia, S. L. Molodtsov, W. Schneider, A. Ionov, M. Richter, and C. Laubschat, J. Alloys Compd. **275-277**, 493 (1998).

[12] A. B. Andrews, J. J. Joyce, A. J. Arko, J. D. Thompson, J. Tang, J. M. Lawrence, and J. C. Hemminger, Phys. Rev. B **51**, 3277 (1995).

[13] W. Schneider, S. L. Molodtsov, M. Richter, Th. Gantz, P. Engelmann, and C. Laubschat, Phys. Rev. B **57**, 14930 (1998).

[14] R. Hayn, Yu. Kucherenko, J. J. Hinarejos, S. L. Molodtsov, and C. Laubschat, Phys. Rev. B **64**, 115106 (2001).

[15] O. K. Andersen, Phys. Rev. B **12**, 3060 (1975).

[16] S. Hüfner, *Photoelectron Spectroscopy* (Springer, Berlin, 1996).

[17] Yu. Kucherenko, M. Finken, S. L. Molodtsov, M. Heber, J. Boysen, C. Laubschat, and G. Behr, Phys. Rev. B **65**, 165119 (2002).

[18] Yu. Kucherenko, M. Finken, S. L. Molodtsov, M. Heber, J. Boysen, G. Behr, and C. Laubschat, Phys. Rev. B **66**, 165438 (2002).